Scintillation Characteristics of Pr:CaF$_2$ Crystals for Charged-particle Detection

Noriaki Kawaguchi,[1][*] Hiromi Kimura,[1] Masaki Akatsuka,[1] Go Okada,[1]
Naoki Kawano,[2] Kentaro Fukuda,[3] and Takayuki Yanagida[1]

[1]Nara Institute of Science and Technology, 8916-5 Takayama-cho, Ikoma, Nara 630-0192, Japan
[2]Akita University, 1-1 Tegata Gakuen-machi, Akita 010-8502, Japan
[3]Tokuyama Corporation, 1-1 Harumi-cho, Shunan, Yamaguchi 745-0024, Japan

The scintillation properties of Pr:CaF$_2$ were studied in comparison with those of Eu:CaF$_2$ under α-ray excitation using a sealed source of ^{241}Am. The relative light yields of the Pr:CaF$_2$ crystals were approximately 0.6–13% of the Eu:CaF$_2$ crystal that is known as a conventional scintillator for charged-particle detection. The scintillation decay times of the Pr:CaF$_2$ crystals were significantly faster than that of the Eu:CaF$_2$ crystal. Therefore, the Pr:CaF$_2$ crystals can be used for charged-particle measurements with high count rates.

1. Introduction

Some phosphors can be used for measurements of ionizing radiation such as X-rays, γ-rays, neutrons, and charged particles. Such phosphors convert ionizing radiation to visible light and are coupled with a conventional photodetector. Inorganic phosphors for radiation measurements can be classified as either scintillators[1] or storage phosphors. Storage phosphors [also known as thermoluminescence,[2] optically stimulated luminescence,[3–6] and radio-photoluminescence[7–11]] are used to record information on radiation dose whereas scintillators immediately convert ionizing radiation to visible light.[12,13] Among these materials, scintillators are particularly suitable for online measurements.

The required characteristics of the scintillator are a high light yield, a fast decay time, and a high discrimination capability. The light yield affects the energy resolution of the scintillation detector, and it is required by some applications. The fast decay time is required because it allows fast responses of scintillation detectors. To discriminate ionizing radiations, the effective atomic number (Z_{eff}) of the scintillator is important. Scintillators for γ-ray detection are required to consist of heavy elements that efficiently interact with γ-rays. In contrast, scintillators for thermal neutron and charged-particle detection are required to consist of light elements in order to decrease the rate of erroneous detection due to the interaction with γ-rays. Additionally, thermal neutron scintillators have to contain elements with high cross sections

for the (n, α) and (n, γ) nuclear reactions (e.g., ^{6}Li or ^{10}B). For charged-particle detection, the most common materials are Ag:ZnS and Eu:CaF$_2$ that contain relatively insensitive elements for both γ-rays and thermal neutrons. The conventional scintillators for γ-ray and thermal neutron detection were reviewed by van Eijk,[12] who comprehensively covered, for example, Tl:NaI, Tl:CsI, Bi$_4$Ge$_3$O$_{12}$, Ce:Gd$_2$SiO$_5$, and Ce:Lu$_2$SiO$_5$ as γ-ray scintillators, and LiF/Ag:ZnS, Eu:LiI, and GS20 (Ce-doped lithium silicate glass) as thermal neutron scintillators. The γ-ray scintillators have high marketability owing to their medical and security applications; therefore, many materials were developed. The Ce:LaBr$_3$[14] and SrI$_2$[15] scintillators, which show extremely high light yields, are recent attractive materials because the energy resolution of the γ-ray detector is important for its applications. In the case of the thermal neutron scintillator, one of the most common materials is the GS20 glass owing to its non-hygroscopicity and acceptable light yield (~6000 photons/neutron). In addition, some new products are available, for example, the Ce:Cs$_2$LiYCl$_6$ single crystal[16] that is hygroscopic but shows high light yield and excellent discrimination capability. Another example is the Eu:LiCaAlF$_6$ single crystal,[17–21] which shows non-hygroscopicity and higher light yield (typically ~20000 photons/ neutron) than GS20. As mentioned above, whereas many γ-ray and thermal neutron scintillators have been developed, relatively few studies were performed for charged-particle scintillators, and thus we are interested in the further study of charged-particle scintillators.

Transition-metal-ion-doped CaF$_2$ crystals are used for the charged-particle scintillators and thermoluminescent materials for radiation dosimetry. Among them, Eu:CaF$_2$ is well known as a commercial scintillator for charged-particle detection. In the α-ray or β-ray measurements (e.g., for dust monitor), erroneous signals by background γ-rays must be suppressed, and in that sense, CaF$_2$ is attractive as a host crystal. The advantage of the Eu:CaF$_2$ crystal is its high light yield, but on the other hand, the disadvantage is its slow decay time. The α/β ratio of the scintillator is also important for charged particle detection. Fluoride materials tend to show a lower α/β ratio than other inorganic materials.[16] Therefore, the Eu:CaF$_2$ crystal is more suitable for β-ray detection than α-ray detection. Other transition-metal-ion-doped CaF$_2$ scintillators have not been studied extensively for α-ray detection, although many dopants (for example, Tm:CaF$_2$, Dy:CaF$_2$, and Mn:CaF$_2$) are studied for radiation dosimetry. The X-ray-induced luminescence and photoluminescence properties of other transition-metal-ion-doped CaF$_2$ have been studied, and it is known that excited Ce^{3+}, Pr^{3+}, and Nd^{3+} ions can emit fast luminescence with the 5d–4f transition.[22–24] The vacuum ultraviolet (VUV) luminescence of Nd^{3+} is the fastest among these ions, but typical photodetectors cannot detect VUV light. Luminescence with the 5d–4f transition of Pr^{3+} ions is faster than that with the 5d–4f transition of Ce^{3+} ions and acceptable wavelength. In this study, we have investigated the α-ray response of Pr:CaF$_2$ crystals.

2. Materials and Methods

The Pr:CaF$_2$ and Eu:CaF$_2$ crystals were prepared by the following method. Starting materials were prepared from a stoichiometric mixture of CaF$_2$ and EuF$_3$ or PrF$_3$ powders (purity < 99.9%) produced by Stella Chemifa Corporation. They were mixed and put into graphite crucibles. The crucibles set in the stainless used steel (SUS) chamber are enclosed by

a carbon heater. The chamber was evacuated up to 10^{-4} Pa. After baking, the chamber was filled with high-purity Ar gas (99.99%) and CF_4 gas (99.99%) until ambient pressure. Then, the crucible was heated up to 1450 °C and kept at this temperature for 30 min and cooled to room temperature. The obtained crystals were cut and polished.

We measured the X-ray-induced emission spectra and transmittance spectra using a spectrometer equipped with a nitrogen-purged sample chamber, a deuterium lamp as a light source, and an X-ray tube as an X-ray source. We also evaluated scintillation decay curves and pulse height spectra under α-ray excitation from a sealed source of ^{241}Am by using a photomultiplier tube (PMT; Hamamatsu, R7600U-200) that is sensitive across the UV and visible wavelength range. Scintillation decay curves were obtained using an oscilloscope (Tektronix, TDS3052C). The obtained decay curves were fitted by

$$I(t) = A_0 + A_1 \exp(-t/\tau_1) + A_2 \exp(-t/\tau_2), \tag{1}$$

where $I(t)$ is the luminescence intensity as a function of time t, τ_1 and τ_2 are the scintillation decay times, and A_0, A_1, and A_2 are constants.

Output signals from the PMT were analyzed using a preamplifier (ORTEC, 113 Scintillation Preamplifier), a shaping amplifier (ORTEC, 672 Spectroscopy Amplifier), and a multichannel analyzer (Amptek, MCA8000A) for the pulse height spectra.

3. Results and Discussion

Figure 1 shows aspects of the cut and polished $Pr:CaF_2$ crystals. All crystal pieces contain no visible cracks and opaque phases. Figure 2 shows the transmittance spectra of the samples. The transmittances at the wavelength of 230–370 nm were more than 80%. Two absorption bands are observed. These bands can be ascribed to the 4f → 5d transition of Pr^{3+}.[25]

Figure 3 shows the X-ray-induced spectra of the $Pr:CaF_2$ and $Eu:CaF_2$ crystals. Emission peaks with the 5d–4f transition of Pr^{3+} or Eu^{2+} ions are observed, and broad peaks are also observed at around 280 nm when the dopant concentrations are low. These broad peaks
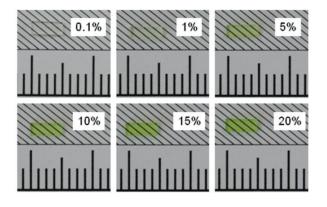

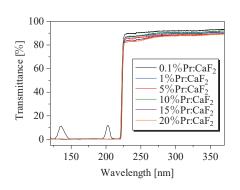Fig. 1. (Color online) Cut and polished $Pr:CaF_2$ crystals.

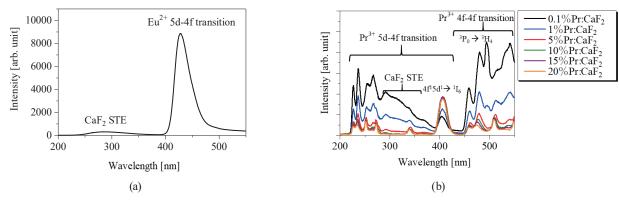Fig. 2. (Color online) Transmittance spectra of $Pr:CaF_2$ crystals.

Fig. 3.   (Color online) Scintillation spectra of (a) Eu:CaF$_2$ and (b) Pr:CaF$_2$ crystals under α-ray irradiation.

indicate the intrinsic luminescence of CaF$_2$ originating from the self-trapped exciton (STE), and these STE emissions are quenched as the Pr^{3+} concentration increased. The emission wavelength of Pr^{3+} ions is overlapped with that of the STE emission of CaF$_2$. The overlapping emission is clearly observed in the case that the Pr^{3+} concentrations are 0.1 and 1%. Emission peaks with the 4f–4f transition of Pr^{3+}ions are also observed from the X-ray-induced spectra of the Pr:CaF$_2$ samples in the wavelength range between 450 and 550 nm. The intensities of these emission peaks are decreased with decreasing Pr^{3+} concentration, and it can be explained by the concentration quenching.

Figure 4 shows the scintillation decay curves of the Pr:CaF$_2$ and Eu:CaF$_2$ crystals under α-ray excitation from the sealed source of ^{241}Am. These decay curves can be fitted by the sum of two exponentials and a constant. The obtained scintillation decay times of the Pr:CaF$_2$ and Eu:CaF$_2$ crystals are shown in Table 1. The scintillation decay curves of the Pr:CaF$_2$ crystals contain both fast and slow components because these are mixed luminescences that originated from the faster 5d–4f transition of Pr^{3+} ions and the slower 4f–4f transition of Pr^{3+} ions or the STE of CaF$_2$. The scintillation decay times of the 5, 10, and 20% Pr:CaF$_2$ crystals are significantly shorter than that of the Eu:CaF$_2$ crystal.

Figure 5 shows pulse height spectra of the Pr:CaF$_2$ crystals under α-ray excitation. Full-energy deposited peaks were obtained by all the samples. Their pulse heights decreased with increasing Pr^{3+} concentration. Figure 6 shows the relative light yields of the Pr:CaF$_2$ crystals calculated from the peak channel numbers of the pulse height spectra of the Pr:CaF$_2$ and Eu:CaF$_2$ under α-ray excitation. Here, we defined the relative light yield of Eu:CaF$_2$ as 1. As a result, the relative light yields of the Pr:CaF$_2$ crystals were around 0.6–13% of that of the Eu:CaF$_2$ crystal. Pr:CaF$_2$ samples with higher dopant concentration show lower light yields because of the concentration quenching of luminescence with the 5d–4f transitions of Pr^{3+} ions.

In summary, the scintillation decay times of the 5, 10, and 20% Pr:CaF$_2$ crystals were significantly faster than that of the Eu:CaF$_2$ crystal. From pulse height spectra under α-ray excitation, full-energy deposited peaks were obtained by all the Pr:CaF$_2$ crystals. Therefore, the Pr:CaF$_2$ crystals can be used for charged-particle measurements with high count rates.
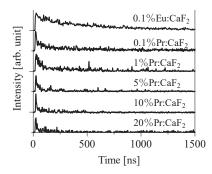
Fig. 4.   Scintillation decay curves of Eu:CaF$_2$ and Pr:CaF$_2$ crystals under α-ray irradiation.

Table 1
Scintillation decay times of Eu:CaF$_2$ and Pr:CaF$_2$ crystals under α-ray irradiation.

	Scintillation decay times (ns)	
	τ_1	τ_2
0.1% Eu:CaF$_2$	140.0	391.2
0.1% Pr:CaF$_2$	36.9	536.8
1% Pr:CaF$_2$	30.9	455.2
5% Pr:CaF$_2$	14.8	284.7
10% Pr:CaF$_2$	6.2	158.2
20% Pr:CaF$_2$	7.5	138.2

Fig. 5.   (Color online) Pulse height spectra of Pr:CaF$_2$ crystals under α-ray irradiation.
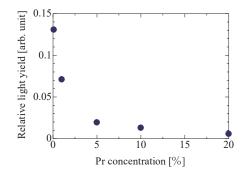

Fig. 6.   (Color online) Dopant concentration dependence of relative light yields (Eu:CaF$_2$ = 1) of Pr:CaF$_2$ crystals under α-ray irradiation.

4.   Conclusions

We have successfully obtained transparent and noncracked crystals of Pr:CaF$_2$. The transmittances of the Pr:CaF$_2$ crystals were more than 80% at the wavelength of 230–370 nm. The Pr^{3+} concentration dependence of X-ray-induced luminescence was investigated. We have confirmed that the STE emission of CaF$_2$ was quenched with increasing Pr^{3+} concentration. The scintillation decay times of the 5, 10, and 20% Pr:CaF$_2$ crystals were shorter than that of Eu:CaF$_2$. The scintillation decay times of high-Pr^{3+}-concentration samples were shorter than those of the other samples. The pulse height spectra of the Pr:CaF$_2$ crystals were measured and full-energy deposited peaks were obtained. The relative light yields of the Pr:CaF$_2$ crystals were around 0.6–13% of the Eu:CaF$_2$ crystal.

Acknowledgments

References

1 G. F. Knoll: Radiation Detection and Measurement (Wiley, New York, 2010) 4th ed.
2 S. W. S. McKeever: Thermoluminescence of Solids (Cambridge University Press, Cambridge, 1985).
3 E. G. Yukihara and S. W. S. McKeever: Optically Stimulated Luminescence (Wiley, Chichester, 2011).
4 S. W. S. McKeever: Nucl. Instrum. Methods Phys. Res., Sect. B **184** (2001) 29.
5 G. Okada, K. Fukuda, S. Kasap, and T. Yanagida: Photonics **3** (2016) 23.
6 N. M. Winch, A. Edgar, and C. M. Bartle: Nucl. Instrum. Methods Phys. Res., Sect. A **763** (2014) 394.
7 H. Nanto, Y. Miyamoto, T. Oono, Y. Takei, T. Kurobori, and T. Yamamoto: Procedia Eng. **25** (2011) 231.
8 G. Okada, B. Morrell, C. Koughia, A. Edgar, C. Varoy, G. Belev, T. Wysokinski, D. Chapman, and S. Kasap: Appl. Phys. Lett. **99** (2011) 121105.
9 G. Okada, J. Ueda, S. Tanabe, G. Belev, T. Wysokinski, D. Chapman, D. Tonchev, and S. Kasap: J. Am. Ceram. Soc. **97** (2014) 2147.
10 Y. Miyamoto, H. Nanto, T. Kurobori, Y. Fujimoto, T. Yanagida, J. Ueda, S. Tanabe, and T. Yamamoto: Radiat. Meas. **71** (2014) 529.
11 G. Okada, Y. Fujimoto, H. Tanaka, S. Kasap, and T. Yanagida: J. Rare Earths **34** (2016) 769.
12 C. W. E. van Eijk: Nucl. Instrum. Methods Phys. Res., Sect. A **460** (2001) 1.
13 T. Yanagida: Opt. Mater. **35** (2013) 1987.
14 E. V. D. van Loef, P. Dorenbos, C. W. E. van Eijk, K. W. Kramer, and H. U. Gudel: Nucl. Instrum. Methods Phys. Res., Sect. A **486** (2002) 254.
15 N. J. Cherepy, G. Hull, A. D. Drobshoff, S. A. Payne, E. Van Loef, C. M. Wilson, K. S. Shah, U. N. Roy, A. Burger, L. A. Boatner, W. S. Choong, and W. W. Moses: Appl. Phys. Lett. **92** (2008) 083508.
16 C. W. E. Van Eijk, A. Bessière, and P. Dorenbos: Nucl. Instrum. Methods Phys. Res., Sect. A **529** (2004) 260.
17 N. Kawaguchi, T. Yanagida, A. Novoselov, K. J. Kim, K. Fukuda, A. Yoshikawa, M. Miyake, and M. Baba: Proc. Nuclear Science Symp., Ed. P. Sellin (IEEE, 2008) 1174–1176.
18 N. Kawaguchi, T. Yanagida, Y. Fujimoto, Y. Yokota, K. Kamada, K. Fukuda, T. Suyama, K. Watanabe, A. Yamazaki, V. Chani, and A. Yoshikawa: Nucl. Instrum. Methods Phys. Res., Sect. A **652** (2011) 351.
19 T. Yanagida, N. Kawaguchi, Y. Fujimoto, K. Fukuda, Y. Yokota, A. Yamazaki, K. Watanabe, J. Pejchal, A. Uritani, T. Iguchi, and A. Yoshikawa: Opt. Mater. **33** (2011) 1243.
20 T. Yanagida, A. Yamaji, N. Kawaguchi, Y. Fujimoto, K. Fukuda, S. Kurosawa, A. Yamazaki, K. Watanabe, Y. Futami, Y. Yokota, A. Uritani, T. Iguchi, A. Yoshikawa, and M. Nikl: Appl. Phys. Express **4** (2011) 106401.
21 T. Yanagida: J. Lumin. **169** (2016) 544.
22 T. Yanagida, Y. Fujimoto, K. Watanabe, K. Fukuda, N. Kawaguchi, Y. Miyamoto, and H. Nanto: Rad. Meas. **71** (2014) 162.
23 K. Y. Loong, G. D. Jones, and R. W. G. Syme: J. Lumin. **53** (1992) 503.
24 F. Nakamura, T. Kato, G. Okada, N. Kawaguchi, K. Fukuda, and T. Yanagida: J. Eur. Ceram. Soc. **37** (2017) 4919.
25 K. D. Oskam, A. J. Houtepen, and A. Meijerink: J. Lumin. **97** (2002) 107.